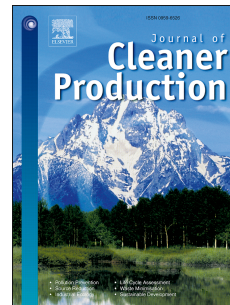


# Accepted Manuscript

A method of strategic evaluation of energy performance of Building Integrated Photovoltaic in the urban context

V. Costanzo, R. Yao, E. Essah, L. Shao, M. Shahrestani, A.C. Oliveira, M. Araz, A. Hepbasli, E. Biyik



PII: S0959-6526(18)30451-7

DOI: [10.1016/j.jclepro.2018.02.139](https://doi.org/10.1016/j.jclepro.2018.02.139)

Reference: JCLP 12086

To appear in: *Journal of Cleaner Production*

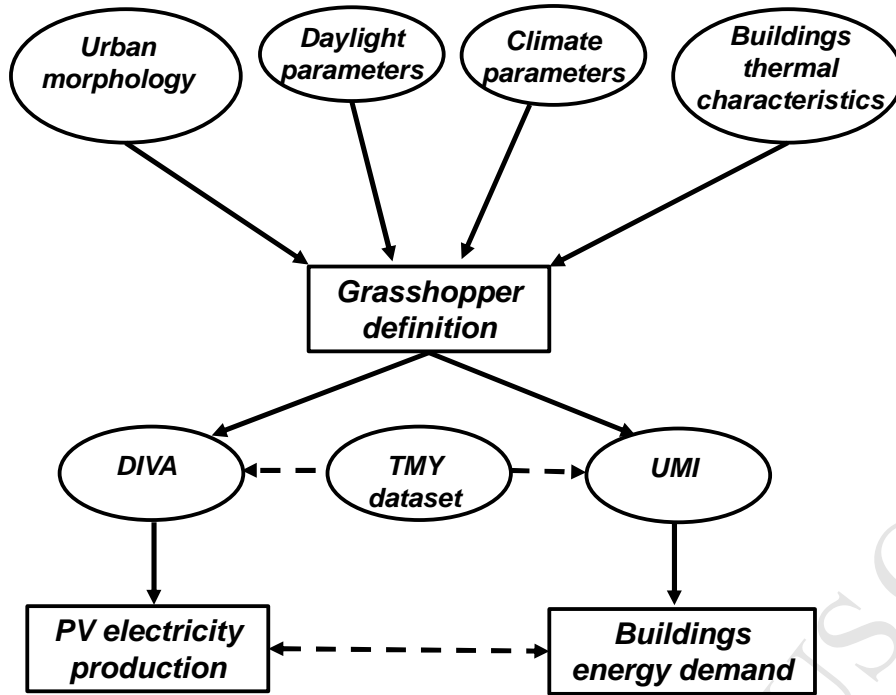
Received Date: 24 November 2017

Revised Date: 2 February 2018

Accepted Date: 13 February 2018

Please cite this article as: Costanzo V, Yao R, Essah E, Shao L, Shahrestani M, Oliveira AC, Araz M, Hepbasli A, Biyik E, A method of strategic evaluation of energy performance of Building Integrated Photovoltaic in the urban context, *Journal of Cleaner Production* (2018), doi: 10.1016/j.jclepro.2018.02.139.

This is a PDF file of an unedited manuscript that has been accepted for publication. As a service to our customers we are providing this early version of the manuscript. The manuscript will undergo copyediting, typesetting, and review of the resulting proof before it is published in its final form. Please note that during the production process errors may be discovered which could affect the content, and all legal disclaimers that apply to the journal pertain.



# A method of strategic evaluation of energy performance of Building Integrated Photovoltaic in the urban context

V. Costanzo<sup>1</sup>, R. Yao<sup>\*1</sup>, E. Essah<sup>1</sup>, L. Shao<sup>1</sup>, M. Shahrestani<sup>1</sup>, A.C. Oliveira<sup>2</sup>, M. Araz<sup>3</sup>, A.  
Hepbasli<sup>3</sup>, E. Biyik<sup>3</sup>

<sup>1</sup>School of the Built Environment, University of Reading, RG6 6AW Reading, UK

<sup>2</sup>Centre for Renewable Energy Research, University of Porto, 4200-465 Porto, Portugal

<sup>3</sup>Department of Energy Systems Engineering, Faculty of Engineering, Yasar University,  
35100 Izmir, Turkey

*\*corresponding author*

Email address: [r.yao@reading.ac.uk](mailto:r.yao@reading.ac.uk)

## Abstract

This paper presents an integrated bottom-up approach aimed at helping those dealing with strategical analysis of installation of Building Integrated Photo Voltaic (BIPV) to estimate the electricity production potential along with the energy needs of urban buildings at the district scale. On the demand side, hourly energy profiles is generated using dynamic building simulation taking into account actual urban morphologies. On the supply side, electricity generated from the system is predicted considering both the direct and indirect components of solar radiation as well as local climate variables. Python-based Algorithm editor Grasshopper is used to interlink four types of modelling and simulation tools as 1) generation of 3-D model, 2) solar radiation analysis, 3) formatting weather files (TMY data set) and 4) dynamic energy demand. The method has been demonstrated for a cluster of 20 buildings located in the Yasar University in Izmir (Turkey), for which it is found the BIPV system could achieve an annual renewable share of 23%, in line with the Renewable Energy Directive target of 20%. Quantitatively-compared demand and supply information at hourly time step shows that only some energy needs can be met by BIPV, so there is a need for an appropriate matching strategy to better exploit the renewable energy potential.

31 **Keywords:** solar potential, urban modelling, BIPV, energy matching, energy supply and  
32 demand

### 33 1. Introduction

34 In the past years, EU Commission put into force the recast version of the Directive on the  
35 Energy Performance of Buildings (EU, 2010) and the Renewable Energy Directive (European  
36 Parliament, 2009) to achieve the targets of: i) reducing greenhouse gas emissions of 20%  
37 relative to 1990 levels, ii) improving the energy efficiency of buildings up to 20% and iii)  
38 increase the share of renewable energy to 20%. All these objectives have to be met by 2020.

39 In EU countries, there are more than 160 million buildings accounting for almost 40% of  
40 primary energy consumption and most of them have been built when no energy efficiency  
41 regulations were into force (iNSPiRe Projects, 2014), so there is a space for renewable and  
42 sustainable energy generation technologies to rapidly spread. Within this context,  
43 photovoltaic (PV) technology is growing quickly compared to other renewables, and Building  
44 Integrated Photo Voltaic (BIPV) in particular. In fact, apart from producing clean energy  
45 directly on-site, architectural integration to roofs and walls may add additional benefits such  
46 as reduced costs of material and labour and improved aesthetic (Baljit et al., 2016).

47 A recent review paper about BIPV systems (Biyik et al., 2017) categorized the existing  
48 literature into 5 different groups: i) building-scale applications and experimental studies, ii)  
49 building-scale simulation and numerical studies, iii) cell/module design studies, iv) grid  
50 integration studies and v) policy and strategies studies.

51 If looking at studies about the use of BIPV panels at district/urban scales, most of the authors  
52 focused on the estimate of the solar potential of roofs and facades following two main  
53 approaches: the use of Digital Surface Models (DSM) and of Laser Imaging Detection and  
54 Ranging (LiDAR) information. An example of DSM application can be found in (Redweik et  
55 al., 2013), where the authors exemplarily analysed the University Campus of Lisbon (Portugal)  
56 to test the capability of their SOL algorithm in estimating solar irradiances on roofs and  
57 facades at one meter spatial resolution and one hour time step. On the other hand, LiDAR  
58 technology has been recently employed by (Martínez-Rubio et al., 2016) in obtaining a  
59 detailed map of solar radiation for roofs and facades of an urban area approximately 80 km<sup>2</sup>  
60 wide in Spain using five minutes irradiance records. More examples, together with a  
61 discussion of the strengths and limitations of different approaches employed to appraise the  
62 solar potential of an urban area, can be found in Section 2.1.

63 Despite several researchers have focused on the topic, not many have tackled the issue of  
64 understanding the matching issues between BIPV electricity production and buildings energy  
65 demand at the cluster level: Brownsword et al. (Brownsword et al., 2005) estimated the PV  
66 resource for roofs application in Leicester city (UK) considering south, south-west and south-  
67 east orientations, fixing the suitable installation area at 75% of total roofs area and a module  
68 efficiency of 10%. Electricity demand data is gathered from two different local sources for an  
69 entire year at half-hourly time step.

70 Similarly, Lund (Lund, 2012) analysed potential applications of PV panels on roofs for the  
71 two very different climates of Shanghai (China) and Helsinki (Finland) assuming 50%  
72 availability of roofs area and neglecting the shading effects. He also proposed different  
73 electricity management strategies, finding that for both the cities analysed electricity-to-  
74 thermal conversion of surplus renewable electricity (i.e. that beyond the self-use of  
75 consumers) outperforms electricity-to-storage and load-renewable production peak matching.  
76 Energy demand data is modelled by using a load distribution function exponentially declining  
77 when moving from the city centre to the outskirts.

78 More recently, Wegertseder et al. (Wegertseder et al., 2016) developed a method that  
79 combined solar mapping of roof surfaces carried out within a GIS environment with energy  
80 consumption patterns of the building stock in Concepción (Chile) modelled running dynamic  
81 simulations in DesignBuilder. Through the definition of typical buildings, the authors were  
82 able to develop different load profiles to be matched with the expected local electricity  
83 production and thus to predict the spatial power flows in the urban electricity grid.

84 Finally, (Brito et al., 2017) carried out a techno-economic analysis of the feasibility of BIPVs  
85 in two different areas in Lisbon (Portugal) by coupling LiDAR and Typical Meteorological  
86 Year (TMY) weather data with the SOL algorithm proposed by (Redweik et al., 2013).  
87 Although accurate on the supply side, the demand side is estimated by means of a top-down  
88 approach by multiplying the estimated number of inhabitants by average per capita electricity  
89 demand. Different scenarios in terms of energy demand, such as the application of energy  
90 conservation measures or different occupancy patterns, cannot be addressed and would rather  
91 need a bottom-up approach (Reinhart and Cerezo Davila, 2016).

92 The aim of this paper is to develop a comprehensive bottom-up approach for helping local  
93 authorities, institutions and engineers understanding the technical potential of BIPV  
94 installations at the scale of cluster of buildings.

95 To this aim, a workflow has been implemented within the Python-based algorithm editor  
96 Grasshopper that interlinks state of the art modelling tools, local climate variables and

97 daylight parameters in order to: i) estimate the energy demand of the institutional buildings  
98 by means of hourly dynamic simulations, ii) rank every surface according to a detailed solar  
99 radiation analysis accounting for both the direct and indirect solar radiation components and  
100 iii) appraise the BIPV yield achievable by the best surfaces.

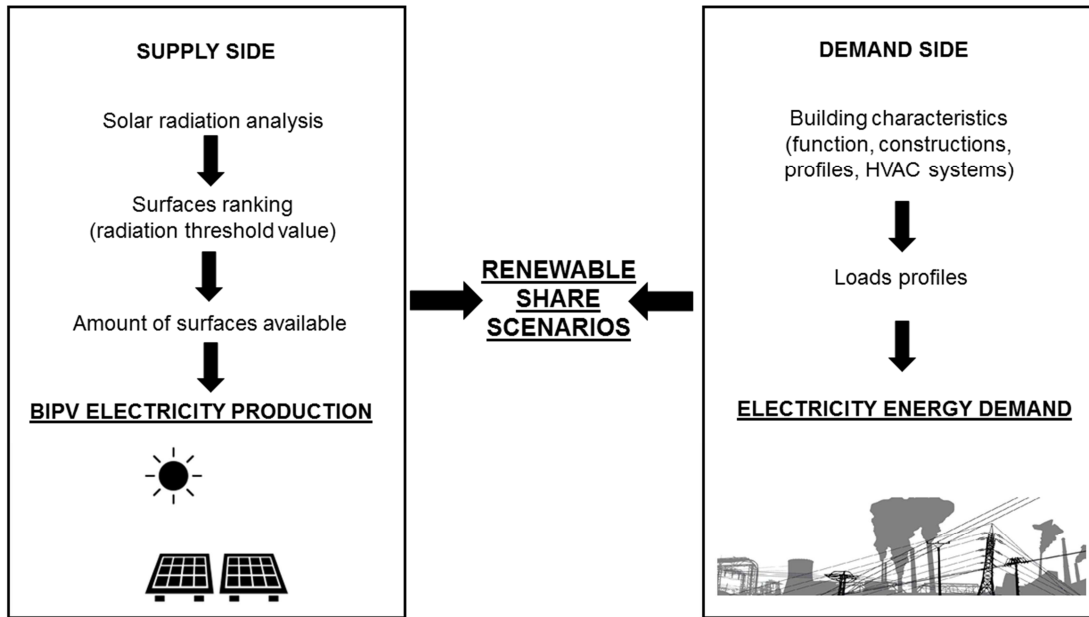
101 In this way, the effect of different supply/demand strategies at the scale of clusters of  
102 buildings can be accounted for, thus greatly helping translate in practice the generic and  
103 nation-wide renewable production and energy efficiency goals set by laws and regulations.

104

## 105 **2. Methodology**

106 The proposed methodology makes use of detailed dynamic simulations to estimate both the  
107 electricity yield from BIPV installed on buildings envelopes (roofs and facades), and the  
108 buildings energy demand. The conceptual framework of Fig. 1 summarizes the main steps of  
109 this process: on the supply side, the solar radiation analysis of buildings surfaces allows to  
110 rank them according to the amount of solar radiation perceived in a year, and then to quantify  
111 the area available for PV installation according to an user-defined radiation threshold. Then,  
112 the electricity yield is estimated by considering also the environmental variables affecting the  
113 electrical efficiency of PV panels. On the demand side, the characterization of the buildings  
114 in terms of function, constructions, occupancy profiles and HVAC systems allows to get the  
115 energy demand profiles for various end-uses and thus their final electricity demand.

116 It is finally possible to compare both the supply and demand profiles in order to study the  
117 feasibility of different renewable share scenarios, as well as the matching issues arising from  
118 the use of a discontinuous energy source like the sun.



119

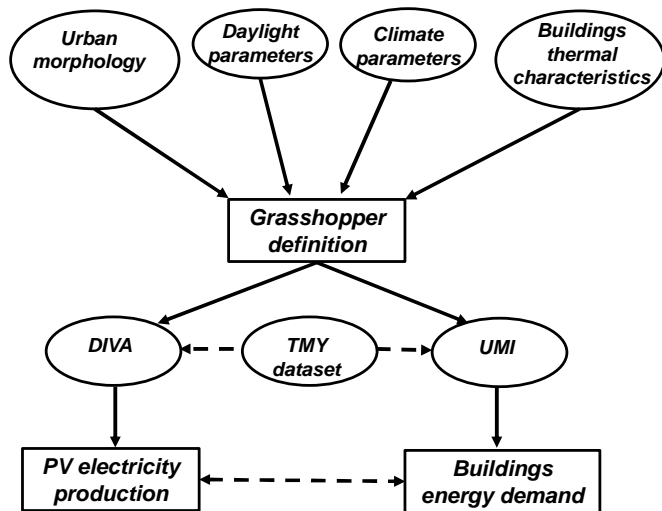
120 Figure 1. Framework of the proposed methodology

121 To accomplish these tasks, several simulation tools are interconnected using the algorithm  
 122 editor Grasshopper (see Fig. 2) that allows the users to write their own Python-based  
 123 definitions (Grasshopper, 2017). In our approach it is used to reference: i) a 3D model of the  
 124 study area, ii) materials optical properties and sky conditions to run surface irradiance  
 125 analysis (daylight parameters), iii) climatic parameters related to the specific site in the  
 126 format of TMY dataset) and iv) building thermal characteristics to run dynamic energy  
 127 simulations. The outputs generated by the different simulation tools are solar irradiance  
 128 values for each surface of the model (DIVA software), PV efficiency values and electricity  
 129 production for the best collecting surfaces (Grasshopper definition), and finally the energy  
 130 needs of the buildings (UMI software).

131 Details for each modelling step outlined above are provided in the next subsections.

132

133



134

135 Figure 2. Data interconnection among the different simulation tools

136

137 *2.1 3D model generation and irradiance analysis*

138 In order to perform a quick analysis of the solar potential of a study area, a 3D model built at  
 139 Level of Detail 1 is employed. According to (Biljecki, 2013), buildings at this level of detail  
 140 are represented as footprint extrusions and with flat roofs. Nonetheless, it is possible to use  
 141 more detailed three-dimensional representations for analysis concerning a limited number of  
 142 buildings since computation time exponentially increases with the number of modelled  
 143 surfaces.

144 Once the physical model is available, two main approaches for estimating solar irradiance  
 145 values on building envelopes can be employed according to the literature review of Freitas et  
 146 al. (Freitas et al., 2015): empirical based or computational based.

147 The *empirical based models* transpose the global and diffuse horizontal radiation values  
 148 measured from weather stations located in open fields into the direct beam and diffuse  
 149 components for any tilted surface by also considering the reflections due to the ground's  
 150 albedo.

151 In general, there is a big consensus around the use of the Perez anisotropic sky model (Perez  
 152 et al., 1987) that considers one direct beam component from the sun, three diffuse sky  
 153 components – deriving from the circumsolar disc close to the sun's position, the horizon  
 154 band close to the ground and the isotropic contribution from the remaining of the sky dome  
 155 respectively – and the ground reflected component. However, these models fail when  
 156 complex urban layouts need to be taken into account, especially when obstructions to sunlight  
 157 can strongly affect solar harvesting like within dense urban environments. Consequently, the

158 development of *computational based models* that mainly differ each other for the resolution  
159 (both spatial and temporal) of the analysis and the radiation components taken into account.  
160 Most of the computational based models available in the literature focus on the appraisal of  
161 the direct and diffuse components only: Erdélyi et al. (Erdélyi et al., 2014) developed a  
162 vectorial-based model called SORAM that augments the anisotropic Perez sky formulation  
163 but is only applicable for flat/tilted roofs. Another vectorial model, based on 2.5D GIS  
164 geometric data of an urban area of Madrid (Spain), has been developed by Esclapés et al.  
165 (Esclapés et al., 2014) and it is able to predict if the study points on both roofs and facades  
166 are sunlit by means of algebraic and trigonometric equations. The most detailed models  
167 developed so far, i.e. those able to account also for the reflected solar radiation component,  
168 made use of different approaches and calculation tools.

169 As an example, De La Flor et al. (De La Flor et al., 2005) developed a characterization  
170 method that relies on the use of an isotropic sky and fixed sun positions for getting irradiance  
171 values on surfaces (roofs and facades) assumed as grey bodies after that a fixed number of  
172 rays cast them according to a deterministic directional distribution.

173 Compagnon (Compagnon, 2004) developed a computer program that used a 2.5D model to  
174 be translated into the Radiance format for running a detailed irradiance analysis on both roofs  
175 and facades. This approach has been tested for a district located in Fribourg (Switzerland),  
176 using the Perez sky formulation and a fixed value for the solar reflectance of every building  
177 surface.

178 Then, Jakubiec and Reinhart (Jakubiec and Reinhart, 2013) enhanced the Radiance based  
179 approach by coupling a detailed 3D GIS model of the city of Cambridge in the US – derived  
180 from LiDAR data – with DAYSIM irradiance hourly simulations. Their approach proved to  
181 be very detailed since a comparison with two existing rooftop installations showed annual  
182 errors less than 5% in terms of electricity production. However, only roofs are considered in  
183 this work.

184 The approach used in this study is computational based and furthers that of Jakubiec and  
185 Reinhart (Jakubiec and Reinhart, 2013) by using the capabilities of Radiance coupled with  
186 the visual interface provided by DIVA (Reinhart et al., 2014) to estimate solar irradiance  
187 values not only on roofs but also on building facades. Radiance is a well validated backward  
188 ray tracer tool (Ward and Rubinstein, 1988) that can use several sky models, from customized  
189 ones to standard CIE models. Because of this capability, hourly climate-based daylight  
190 simulations are carried out using the daylight coefficient approach implemented by

191 Mardaljevic (Mardaljevic, 2000) for the already mentioned Perez's sky model (Perez et al.,  
192 1987).

193 Another noticeable difference between the approach implemented here and that of (Jakubiec  
194 and Reinhart, 2013) is given by the use of a 3D model built within the Rhino CAD  
195 environment. Rhino is a powerful tool that allows modelling geometries of every complexity  
196 as well as to import different file formats and convert them into the .3dm proprietary format.  
197 This means a high user flexibility because it is possible to import a physical model already  
198 available in other formats as well as to create a new one, thus bypassing the need for a GIS  
199 model that very often is available only for few big cities in the world.

200 The model is then referenced as a closed boundary representation (*brep*) and passed to  
201 Grasshopper where every surface is manipulated and characterized by assigning different  
202 optical and thermal properties.

203 Finally, the results of the simulations are shown in a false-colour scale showing both the  
204 amount of solar energy perceived by every surface as well as the extent of the surfaces  
205 receiving more than a user-defined threshold value. This will greatly help in highlighting the  
206 best surfaces for PV panels' installation, for which the calculation of the electricity  
207 production detailed in the following can be performed.

208

## 209 2.2 PV panels' efficiency and electricity yields calculation

210 In the literature, several approaches have been employed for estimating PV efficiency  
211 variations due to different panel technologies (Mono-c-Si, Multi-c-Si, a-Si, CIGS, CdTe),  
212 mounting layout (i.e. free racks, roof mounted, building integrated) and operational  
213 conditions.

214 As reported by (Mattei et al., 2006), the most used model is represented by the following  
215 algebraic equation:

$$216 \quad \eta_{PV} = \eta_{ref} [1 - \beta(T_c - T_{ref}) + \gamma \text{Log}I] \quad (1)$$

217 where the electrical efficiency  $\eta_{PV}$  is related to the reference value  $\eta_{ref}$  provided by the  
218 manufacturer under Standard Reporting Conditions (SRC), that is to say  $T_{ref} = 25^\circ\text{C}$  and a  
219 solar irradiance value  $I_{ref} = 1000 \text{ W m}^{-2}$  impinging on the panel surface (the G 173 solar  
220 irradiance spectrum distribution is usually used (ASTM G173-03, 2012)).  $\beta$  and  $\gamma$  are the  
221 efficiency correction coefficients for cell temperatures and irradiance levels others than the  
222 standard ones, respectively, and depend on the material used for making the panel.

223 As an indication,  $\beta$  ranges from  $-0.25\%^{\circ}\text{C}^{-1}$  for CdTe panels to  $-0.45\%^{\circ}\text{C}^{-1}$  for Multi-c-Si  
224 panels, while  $\gamma$  ranges from 0.085 for Mono-c-Si installations to 0.12 for Multi-c-Si ones.

225 The previous equation is usually simplified by neglecting the explicit irradiance term  $\gamma \text{Log}I$   
226 without losing accuracy since the irradiance effect is implicitly taken into account by the cell  
227 temperature  $T_c$ .

228 An established way to obtain  $T_c$  ( $^{\circ}\text{C}$ ) via an energy balance on the module makes use of the  
229 so-called Nominal Operating Cell Temperature (NOCT). It is defined as the panel  
230 temperature reached under Nominal Terrestrial Environment (NTE) conditions, let's say  
231 global solar irradiance  $I = 800 \text{ Wm}^{-2}$ , ambient temperature  $T_a = 20^{\circ}\text{C}$ , average wind speed of  
232  $1 \text{ ms}^{-1}$  (without considering any wind direction), no electrical load and free rack installations  
233 facing normal to noon. Under these conditions, the cell temperature can be expressed as:

$$234 \quad T_c = T_a + (\text{NOCT} - 20) \frac{I}{800} \quad (2)$$

235 Again, NOCT values depend on the material used for making the panels and span from  $43^{\circ}\text{C}$   
236 for Mono-c-Si types to  $47^{\circ}\text{C}$  for CIGS ones. However, this equation is rigorously applicable  
237 only to free rack installation, and cannot be used for BIPV applications as for this study. In  
238 fact, since the two sides of the modules experience quite different ambient conditions, new  
239 prediction approaches have to be sought.

240 If focusing on PV installations on building facades, the problem is further complicated by the  
241 nature of the environment surrounding the facades that alters the wind flow pattern and thus  
242 the magnitude of the heat exchanged by convection.

243 The determination of these losses is usually accounted for either by using convection heat  
244 transfer coefficients that are experimentally or theoretically derived (a thorough review of  
245 wind convection coefficient correlations useful for building envelope calculations is provided  
246 in (Palyvos, 2008)) or by running Computational Fluid Dynamics (CFD) analyses, the last  
247 ones being too time consuming and easily prone to errors to be carried out at urban scale.

248 Schwingshackl et al. (Schwingshackl et al., 2013) tested eight different models to specifically  
249 predict cell temperatures, and found out that it is not possible to identify just one model able  
250 to accurately calculate panel temperatures and their efficiency under different operating  
251 conditions. However, the models including wind speed as a variable generally report better  
252 agreement with experimental measurements.

253 A detailed formulation accounting for air forced convection, natural convection and radiation  
254 losses in free standing PV installations has been developed by Kaplani and Kaplanis (Kaplani

255 and Kaplanis, 2014) and allows to predict the cell temperature as a function of the ambient  
 256 temperature and incident solar radiation on the panel:

$$257 \quad T_c = T_a + fI \quad (3)$$

258 Here,  $f$  is an empirical coefficient, already addressed by other authors and firstly introduced  
 259 by Ross (Ross, R. G., 1976), which is estimated in relation to the overall heat losses of the  
 260 panel.

261 An accurate and easy to use extension of this approach to BIPV installations in urban  
 262 environments is that provided in ref. (Skoplaki et al., 2008): first, a mounting coefficient  $\omega$  is  
 263 defined as the ratio of the Ross' parameter for the specific mounting arrangement to that valid  
 264 for the free rack case (the values taken by the mounting coefficient range from 1 for  
 265 freestanding installations to 2.6 for façade-integrated installations):

$$266 \quad \omega = \frac{f_{mounting}}{f_{free\_rack}} \quad (4)$$

267 Then, the wind convection coefficient is computed by making use of the well-known  
 268 Loveday-Taki relation (Loveday and Taki, 1996):

$$269 \quad h_w = 8.91 + 2.0v_f \quad (5)$$

270 and finally the cell temperature is estimated by the following equation:

$$271 \quad T_c = T_a + \omega \left( \frac{0.32}{8.91 + 2.0v_f} \right) I \quad (6)$$

272 This relation holds for every mounting type and for free wind velocities  $v_f$ , that is to say those  
 273 got by measurements taken at a mast-mounted anemometer well above the PV array.

274 The method developed in this paper makes use of Eq. (6) to estimate cell temperature values  
 275 but slightly modifies it to account for the effect of the urban environment in lowering the  
 276 wind speeds as gathered from meteorological datasets provided in the TMY format (Wilcox  
 277 and Marion, 2008). This task is accomplished by using the traditional power law formulation  
 278 (ASHRAE, 2005) and defining an urban-scaled wind velocity  $v_f^*$  ( $\text{ms}^{-1}$ ):

$$279 \quad v_f^* = v_{met} \left( \frac{\delta_{met}}{z_{met}} \right)^{\alpha_{met}} \left( \frac{z}{\delta} \right)^{\alpha} \quad (7)$$

280 Here,  $v_{met}$  and  $z_{met}$  are respectively the wind velocity and the height above the ground  
 281 (typically 10m) of the local weather station,  $z$  is the height for which the calculation is  
 282 performed and  $\delta$  and  $\alpha$  are the boundary layer thickness and local terrain exponent  
 283 coefficients. Typical values for the last ones are provided in (ASHRAE, 2005).

284 Finally, by combining Eq. (1) with Eq. (6) and considering also the losses due to power  
285 mismatch among the panels and those due to inverter operation by means of the mismatch  
286 and inverter efficiencies  $\eta_m$  and  $\eta_{inv}$  (their values are typically around 0.97 and 0.95  
287 respectively and are provided by the manufacturers), the electrical yield of the effective PV  
288 panel collecting area  $A_{eff}$  is calculated at an hourly time step with the following relation:

$$289 \quad P = \eta_{pv} \eta_m \eta_{inv} A_{eff} I \quad (8)$$

### 290 *2.3 Buildings' load profiles calculation*

291 It is frequent the case when detailed data about the energy demand of buildings, in terms of  
292 hourly profile and breakdown of its components (cooling, heating, lighting and other  
293 equipment), is neither available nor practical to obtain. In such cases, especially at the scale  
294 of clusters of buildings, it is convenient to rely on dynamic thermal simulations to get this  
295 comprehensive information.

296 The devised methodology define buildings' load profiles by means of detailed dynamic  
297 simulations carried out using a recently-developed Urban Modelling Interface (UMI)  
298 (Reinhart et al., 2013) that has EnergyPlus v8.1 (EnergyPlus, 2017) as its core engine.

299 By referencing the same 3D urban model created for the solar irradiation analysis, the tool  
300 asks for all the data needed for running traditional EnergyPlus simulations: construction  
301 details, occupancy schedules, internal gains and HVAC characteristics. This piece of  
302 information is then attached to every building as a template. The burden of collecting all the  
303 data needed is counterbalanced by reduced simulation times, since UMI uses an algorithm  
304 able to split the buildings into representative thermal zones according to the definition of  
305 perimeter and core zones reported in the ASHRAE 90.1 Appendix G (ANSI/ASHRAE,  
306 2002). The details of this procedure can be found in (Dogan et al., 2015), where validation  
307 tests show mean percentage errors between 2-5% when the annual energy demand is  
308 compared against the results of traditional EnergyPlus whole-building simulations.

309 The benefits are a strong reduction of simulation times that allows considering a big number  
310 of buildings in the analysis, and the capability of outputting detailed hourly profiles of the  
311 energy demand split into its heating, cooling, lighting and equipment components for every  
312 single building. Although the software itself reports on the electricity demand, it is possible to  
313 consider different energy vectors by inputting the appropriate energy conversion efficiencies  
314 so that different scenarios can be easily appraised (e.g. the choice between gas-fired boilers or  
315 heat pumps for space heating).

316

### 3 Implementation of the developed method – A case study at Yasar University

This section demonstrates the method for the case study of the Yasar University Campus in Izmir (Turkey). First, an overview of the local climate characteristics and campus layout is given, then calculations are performed for all the buildings and the outcomes of the modelling including one exemplary case will be discussed.

#### 3.1 Yasar University case study

Izmir is a city located in the western coastline of Turkey (LAT 38°30'N, LON 27°1'E) that faces the Aegean Sea and whose climate is classified as warm-humid according to ASHRAE Standards 90.1-2004 and 90.2-2004 (ASHRAE, 2004a-2004b), with 1408 HDD and 983 CDD annually calculated on a baseline of 18.3°C (ASHRAE, 2009).

Daily average outdoor temperatures are around 25°C in summer (June to September) and 10°C in winter (December to February), while the corresponding average relative humidity values are 55% and 73% respectively. For what concerns solar radiation, the highest global radiation values are reached by surfaces exposed due south within  $\pm 45^\circ$  tolerance, the main contribution being that of the direct radiation component (see radiation roses in Fig. 3).

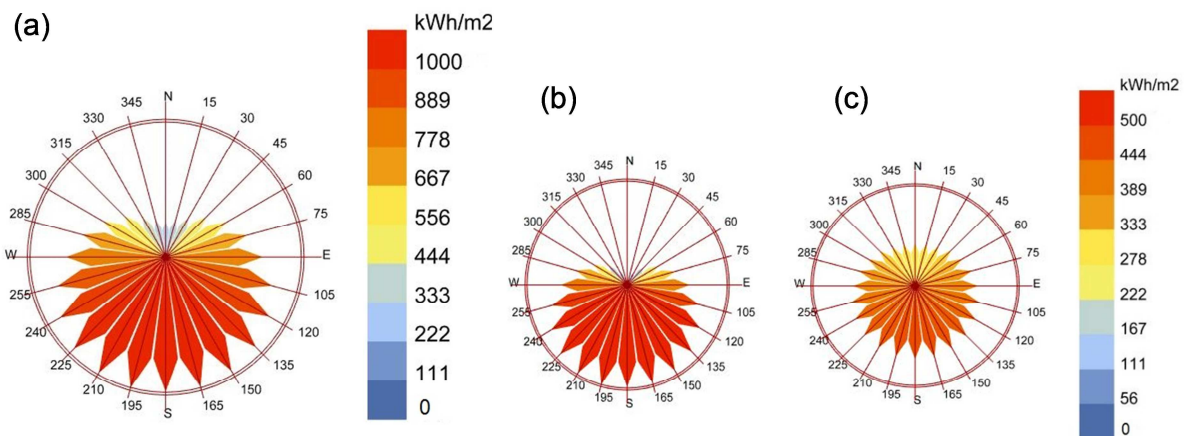
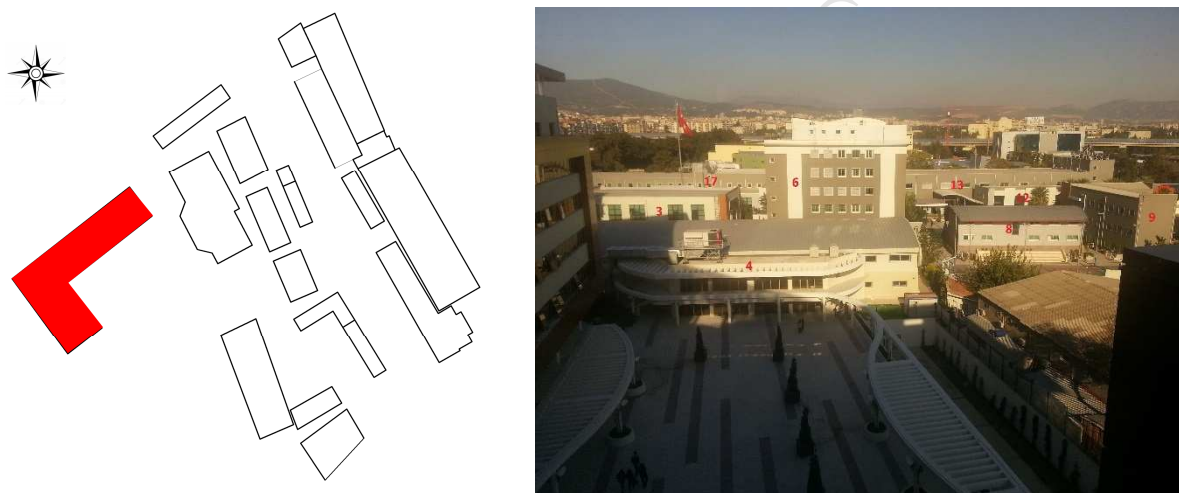


Figure 3. Radiation roses for Izmir: (a) total radiation, (b) direct radiation and (c) diffuse radiation

The Yasar University Campus, located in the Bornova district, is made up of 18 buildings used for academic purposes (classrooms, offices, recreational services) while other buildings are used for hosting mechanical devices and other equipment. Fig. 4 shows a plan and frontal

341 view of the campus buildings, with highlighted in red the building chosen for further detailed  
 342 analysis. This building hosts classrooms that are usually occupied by students from 8:30 AM  
 343 to 6:30 PM, whereas offices are used by staff members from 8:30 AM to 5:30 PM, Monday  
 344 to Friday. Electricity consumption due to internal lighting and various equipments (printers,  
 345 desktop computers and other amenities) amounts to  $8 \text{ Whm}^{-2}$  and  $24 \text{ Whm}^{-2}$  respectively.  
 346 The low energy demand for heating is delivered by gas-fired boilers, whereas a chiller with  
 347 an average coefficient of performance of 4.86 provides space cooling. As for the  
 348 constructions, metal sandwich panels filled with rockwool insulation are used for both the  
 349 external walls (U-value of  $0.35 \text{ Wm}^{-2}\text{K}^{-1}$ ) and the roof (U-value of  $0.5 \text{ Wm}^{-2}\text{K}^{-1}$ ). Windows  
 350 are double-glazed aluminum framed with an air gap and an external reflective coating (visible  
 351 transmittance value of 0.57) with a resulting U-value of  $2.8 \text{ Wm}^{-2}\text{K}^{-1}$ .



352  
 353 Figure 4. Plan view of the campus with the test building highlighted in red (on the left) and  
 354 frontal view of some of the campus buildings (on the right)

355

### 356 *3.2 Solar availability analysis and expected BIPV electricity yield from facades*

357 Annual simulations have been performed in order to evaluate the amount of solar radiation  
 358 impinging on each surface of the buildings at an hourly time step using the DIVA software  
 359 (DIVA, 2017). In order to keep a good spatial resolution within reasonable simulation times,  
 360 a mesh dimension of  $1.5 \times 1.5 \text{ m}^2$  has been chosen for the sensor nodes placed on the surfaces  
 361 with their normal facing outwards. The solar reflectance values of ground, facades and roofs  
 362 are set to 0.20, 0.35 and 0.30 respectively. As for the Radiance parameters, preliminary  
 363 sensitivity analysis allowed to choose the values listed in Table 1 for running the simulations.  
 364 In particular, higher ambient bounces (*ab*) values have been explored to assess their influence  
 365 on the reflected component calculation. This exercise demonstrated that using higher *ab*

366 values (up to 5) would lead to negligible differences in the estimated annual perceived  
 367 radiation (less than 5%), but at the expense of much higher simulation times (up to three  
 368 times).

369

370 Table 1. Radiance parameters

$ab$	$ad$	$as$	$ar$	$aa$
3	1000	20	300	0.1

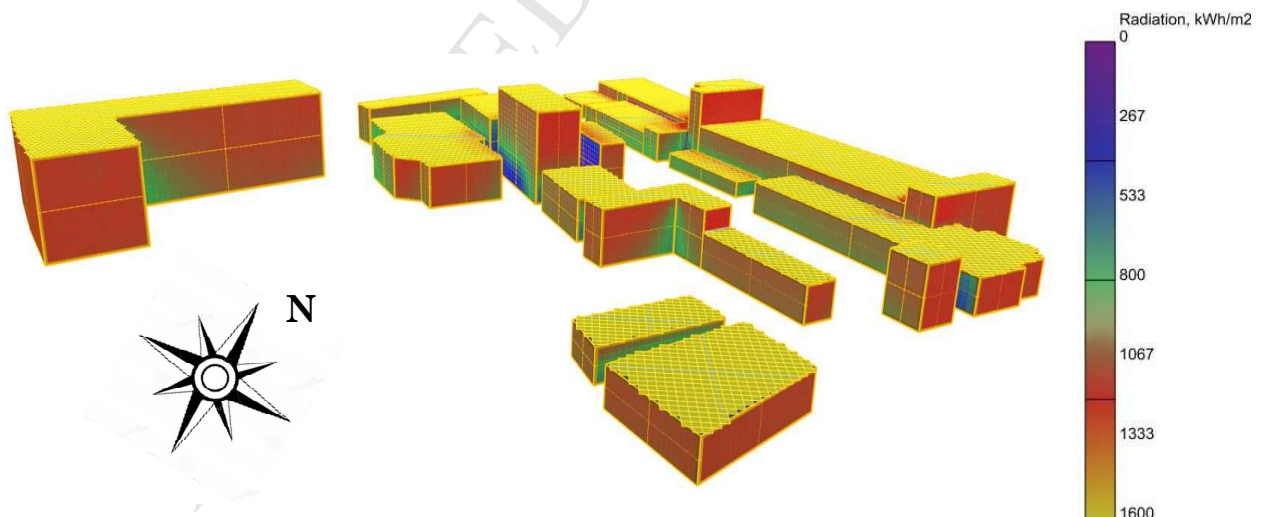
371

372 Simulations have been carried out also by neglecting the reflected component ( $ab = 0$ ); in this  
 373 case, differences up to minus 60% could be expected in the amount of the solar radiation  
 374 perceived by surfaces shaded by the surroundings, irrespective of their orientation. This  
 375 rebates the need for a detailed radiation analysis that accounts for reflections among several  
 376 facades within an urban environment.

377 Finally, annual cumulative solar radiation values have been plotted on the 3D model of the  
 378 campus as surface-averaged values on a false-colour scale with the aim of showing the most  
 379 suitable surfaces for BIPV application.

380 From this analysis (see Fig. 5) it emerges how, apart from the mutual shading effects due to  
 381 the buildings layout, the most suitable vertical surfaces are those facing the south/south-west  
 382 directions.

383



384

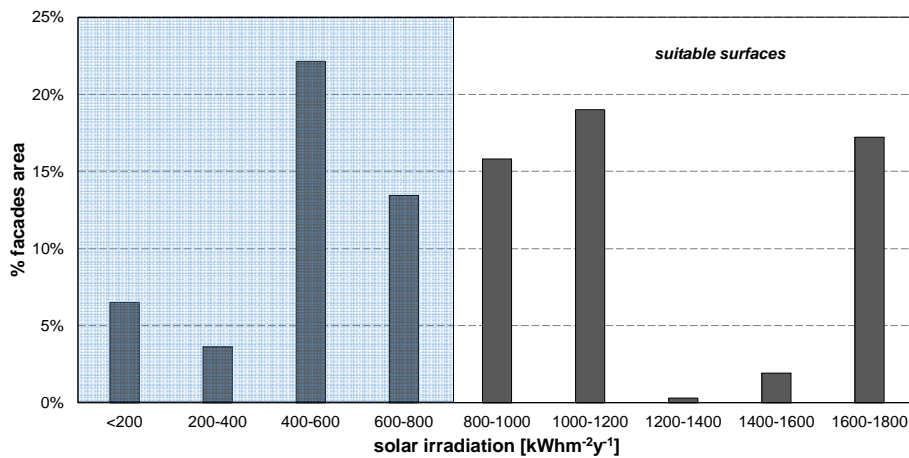
385 Figure 5. Annual cumulative solar radiation values for the campus buildings

386

387 However, not all of these facades (around 21720 m<sup>2</sup>) are adequate to host PV panels: in order  
 388 to rank them, a solar radiation threshold value needs to be defined. According to Compagnon  
 389 (Compagnon, 2004), this threshold has been set to 800 kWhm<sup>-2</sup>y<sup>-1</sup>, making the potential

390 surfaces amount equal to 11790 m<sup>2</sup> (i.e. the sum of the suitable surfaces listed in Fig. 6  
 391 according to their perceived solar radiation).

392



393

394 Figure 6. Ranking of facades area according to the perceived annual solar radiation

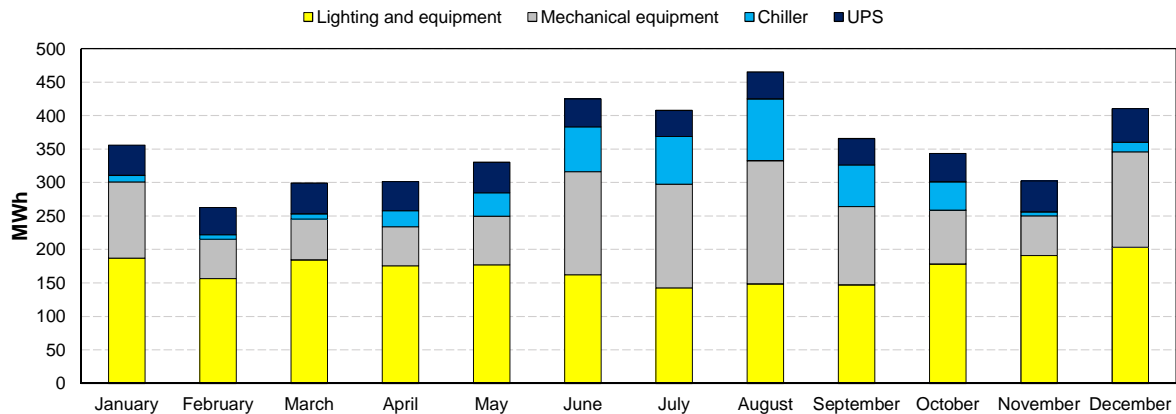
395 Further reductions have to be considered for accounting of windows, protrusions or technical  
 396 services that limit PV applications to facades: the only reference value found in the literature  
 397 suggests a 20% reduction due to balconies and alcoves (Fath et al., 2015). This value has  
 398 been incremented up to 50% for considering also the space occupied by windows, assuming a  
 399 fixed window to wall ratio of 0.3. In the end, the amount of facades that are suitable for BIPV  
 400 installations equals to 5895 m<sup>2</sup>, which represent 27% of the total facades area. By using the  
 401 technical specifications for the photovoltaic panels installed on the same exemplary building  
 402 of this study by Shahrestani et al. (Shahrestani et al., 2017), the expected annual electricity  
 403 delivery from BIPV panels on facades only has been calculated using Eq. (8) and amounts to  
 404 1010 MWh. This equals to a reduction in carbon emissions of approximately 495 tCO<sub>2</sub>, as  
 405 calculated according to the carbon emission factor reported in (Turkey energy efficient report,  
 406 2011).

407

### 408 3.3 Buildings energy demand

409 University campus management staff measured the electricity consumption due to  
 410 interior/exterior lighting, appliances and mechanical equipment for all the campus buildings  
 411 on a monthly basis throughout the year 2016 from the local electricity transformer. These  
 412 values are reported in Fig. 7, and amounts to an annual consumption of 4270 MWh, thus  
 413 making the share of electricity needs that can be annually supplied by BIPV under the  
 414 business as usual scenario around 23%.

415



416

417 Figure 7. Measured monthly electricity consumption of the campus

418

419 This result is considered very positive since it allows to comply with the Renewable Energy  
 420 Directive that prescribes, among the others, to cover at least 20% of the energy needs by  
 421 means of renewable sources by 2020 (European Parliament, 2009). However, if more  
 422 ambitious scenarios should be implemented by considering electricity production from PV  
 423 panels only, additional suitable surfaces may be sought. In this sense, roofs represent the  
 424 most obvious choice because of the large amount of surfaces available and of the higher  
 425 radiation values reached as shown in Fig. 5. Nonetheless, it is worth to mention that surface  
 426 reductions should be considered as well for installations on flat roofs, especially when other  
 427 green building strategies such as green roofs have to be accommodated (Tong et al., 2016).

428

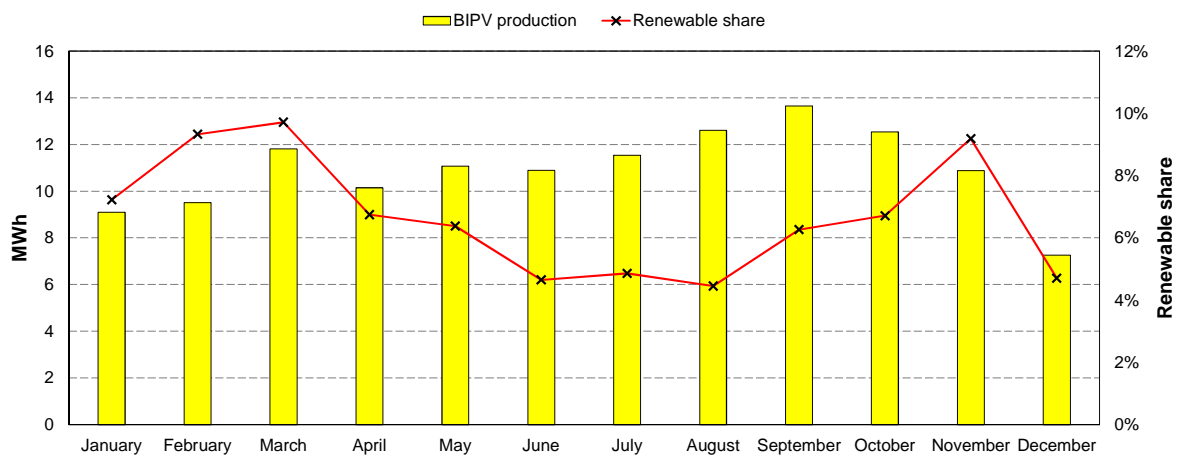
#### 429 *3.4 Demand and supply matching for an exemplary building*

430 A finer level of detail at both spatial and temporal scales is needed when dealing with the  
 431 energy supply from discontinuous energy resources such as solar and wind in order to predict  
 432 with reasonable accuracy the matching issues between energy supply and demand.

433 The proposed method allows reaching a temporal resolution of one hour on both the supply  
 434 and demand side calculation steps. Based on the monthly measured energy consumption of  
 435 the campus previously discussed, a calibrated energy model of the campus buildings has been  
 436 developed in UMI making use of the same 3D model built for the irradiation analysis.

437 For the sake of showing the importance of considering simultaneously both the single  
 438 building scale and that of clusters, the matching issues are here discussed for the exemplary  
 439 building highlighted in Fig. 4. This building mainly hosts classrooms throughout the year and

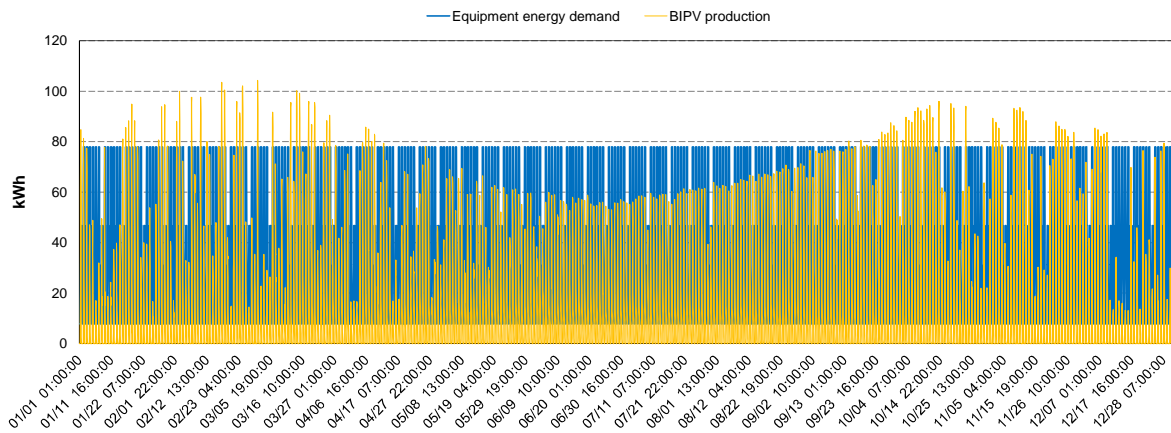
440 it is the most energy consuming of the campus, with a monthly peak electricity consumption  
 441 of around 14 MWh in September (see Fig. 8). According to the solar radiation analysis  
 442 carried out previously, a suitable area of 1302 m<sup>2</sup> could be successfully used for BIPV  
 443 application, which leads to the monthly renewable shares (i.e. the share of the total electricity  
 444 demand deliverable by photovoltaics) depicted in Fig. 8 on the secondary y-axis. This  
 445 monthly supply profile shows that the peak electricity production from BIPV occurs from  
 446 August to October, because of the higher solar radiation values and of the more favourable  
 447 solar height. Nevertheless, the maximum renewable share achievable is around 10%, meaning  
 448 that the remaining electricity demand has to be delivered by the grid or by an oversupply  
 449 from other buildings of the same cluster.  
 450



451  
 452 Figure 8. Monthly BIPV electricity production (yellow bars) and share of energy demand (red  
 453 line) covered by BIPV for the test building

454  
 455 A way to better exploit the electricity production potential from BIPV could thus be that of  
 456 covering just one or more final energy uses. A breakdown of the electricity demand showed  
 457 that electrical equipment, including plug loads and artificial lights, have a magnitude  
 458 comparable to that of BIPV electricity yield in terms of kWh. Fig. 9 shows the hourly profiles  
 459 of the energy demand for electrical equipment (blue line) and of the BIPV electricity  
 460 production (orange line). According to the monthly supply profile discussed above, peak  
 461 power production occurs when the solar height is more favourable, i.e. during summer and  
 462 transition months, but of course it shows a discontinuous trend. On the other hand, energy  
 463 uses related with electrical equipment keep almost constant throughout the year. In fact, a  
 464 three-step profile characterizes weekdays (around 8 kWh from 10 PM to 7 AM, up to 80 kWh

465 from 8 AM to 6 PM and down to around 50 kWh from 7 PM to 9 PM), while a constant  
 466 demand of 8 kWh can be assumed for the weekends when just some equipment is on stand-by  
 467 mode (see Fig. 9).



468

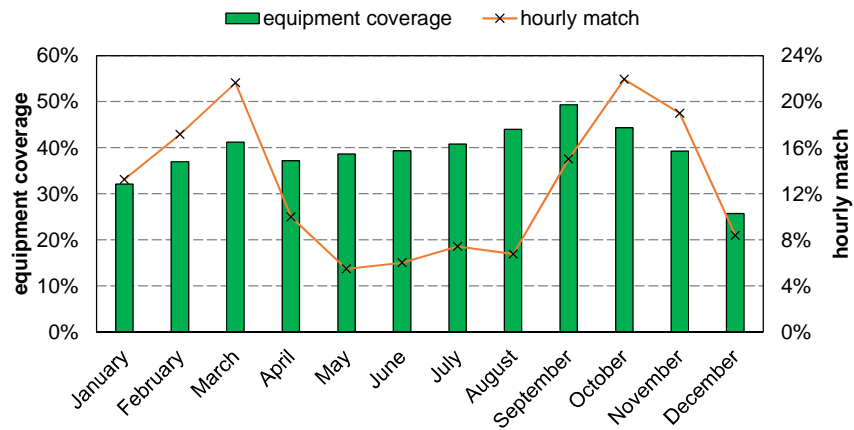
469 Figure 9. Hourly equipment energy demand and BIPV electricity production of the test  
 470 building

471

472 From this hourly representation, it is easy to notice how seldom the peak demand is matched  
 473 by BIPV. A finer analysis of the matching issues is reported in Fig. 10 where the monthly  
 474 coverage of the equipment demand from BIPV (green bars, primary y-axis) is plotted against  
 475 the percentage of hourly matching per month (orange line, secondary y-axis), calculated  
 476 during the period 8 AM to 6 PM in order to not account for those hours without solar  
 477 radiation. The outcomes of this analysis show that, in spite of monthly coverage values up to  
 478 50% (in terms of cumulative electricity demand and supply), BIPV can effectively match the  
 479 equipment demand on an hourly basis for less than 22% of the time under peak production  
 480 conditions.

481 The resolution provided from the simulation framework developed can then inform about the  
 482 adoption of different strategies such as i) supply from the grid, ii) BIPV supply from nearby  
 483 buildings and iii) adoption of a storage system (to be designed according to a carefully  
 484 chosen electricity demand threshold to avoid oversizing and malfunctioning).

485



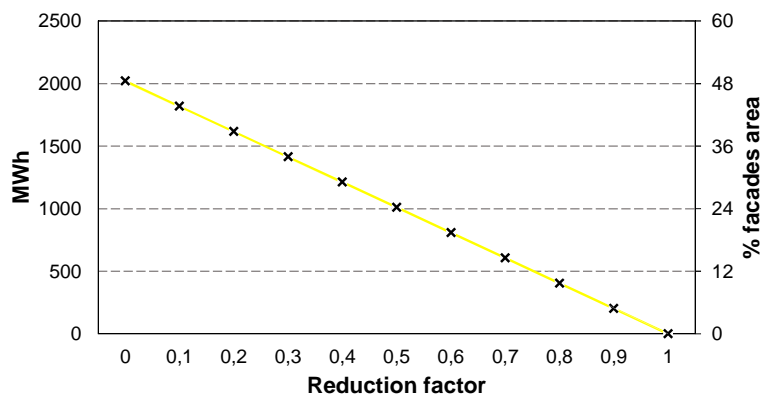
486  
 487 Figure 10. Monthly equipment demand coverage ( bars) and hourly matching occurrences (   
 488 line) for the test building

489

#### 490 4 Discussion

491 The method introduced in this paper first helps identifying and quantifying the amount of  
 492 facades area deemed suitable for PV installation according to an annual solar radiation  
 493 threshold. In the literature, there is a wide consensus around the adoption of the values  
 494 suggested by Compagnon (Compagnon, 2004) for both facades ( $800 \text{ kWhm}^{-2}$ ) and roofs  
 495 ( $1000 \text{ kWhm}^{-2}$ ) because they reflect the technological features of photovoltaic panels  
 496 currently available on the market. Nevertheless, by analysing Fig. 6, it is possible to estimate  
 497 the variation of the suitable surfaces amount due to the adoption of different irradiation  
 498 threshold values. As an example, a decrease of this value from  $800 \text{ kWhm}^{-2}$  to  $600 \text{ kWhm}^{-2}$   
 499 due to technological improvements leads to an increase in the suitable facades area of around  
 500 7%, and to a renewable share of around 27% against the original value of 23%. Although not  
 501 negligible, this difference is less than 5% and no significant improvements in the electricity  
 502 yield are expected when changing the solar radiation threshold to a reasonable lower or  
 503 higher value. On the contrary, changes in the reduction factor of facades due to real urban  
 504 morphology, geometric and technical constraints strongly affect the expected electricity  
 505 yield: the sensitivity analysis carried out in Fig. 11 shows a linear relationship with a slope of  
 506 around  $-20 \text{ MWh}$  per percent increase of the reduction factor. These differences, apart from  
 507 being site-related, also depend on the level of detail of the 3D model of the study area: the  
 508 finer the model, the bigger is the accuracy in the electricity yield estimate and the lower the  
 509 need to rely on reduction factors.

510



511

512 Figure 11. Electricity yield as a function of reduction factor and resulting facades area

513

514 Moreover, it is worth to mention how the optical properties (solar reflectance values namely)  
 515 used for characterizing the urban surfaces are typical of highly urbanized contexts (see  
 516 Section 3.2), and are not expected to affect the outcomes of the calculations in a significant  
 517 way. However, under particular circumstances - such as when the buildings are surrounded  
 518 by green areas, water surfaces or by glazed surfaces - these parameters should be changed  
 519 accordingly.

520 Finally, it is important to state that an economic analysis of the investment profitability is out  
 521 of the scopes of this paper. The reader can refer to the work of (Cucchiella et al., 2015) for a  
 522 comprehensive technical-economic analysis involving the use of several indicators (net  
 523 present value, internal rate of return, discounted payback period, discounted aggregate cost-  
 524 benefit ratio and reduction of carbon dioxide emissions namely), and to that of (Kim et al.,  
 525 2017) for the optimal installation timing of BIPV when considering variations in electricity  
 526 prices.

527

## 528 5 Conclusions

529 This paper presents a comprehensive method intended to help institutional decision makers  
 530 and engineers in addressing the technical feasibility of Building Integrated Photovoltaic  
 531 (BIPV) applications for urban buildings. This bottom-up methodology advances current  
 532 studies on the same topic by coupling state of the art simulation tools to allow a direct  
 533 comparison between the electricity production from BIPV (supply side) and the energy needs  
 534 (demand side) of urban buildings at a district scale and at an hour time step.

535 More in detail, after the creation of a three-dimensional representation of the study area, a  
536 detailed hourly-based solar radiation analysis is performed by means of Radiance  
537 simulations. The outcomes of this analysis are plotted in the model in order to show and  
538 quantify the most suitable surfaces for photovoltaic applications. Solar radiation values are  
539 then coupled with other environmental parameters derived from Typical Meteorological Year  
540 (TMY) dataset and processed in Grasshopper for estimating the electricity production from  
541 BIPV. Finally, thermal simulations using the EnergyPlus software are run for every study  
542 building in order to get the energy consumption profile. Comparison between supply and  
543 demands informs about the best strategy to adopt to achieve the targeted renewable energy  
544 shares.

545 The implementation of the method for the case study of Yasar University campus (Turkey)  
546 revealed that around 27% of façades area is suitable for BIPV installations. This leads to a  
547 renewable share cover, i.e. the amount of total annual electricity needs that can be supplied  
548 by photovoltaic, of about 23% under a business as usual scenario. This result is considered  
549 very positive and comply with the Renewable Energy Directive in force in Europe  
550 prescribing a 20% renewable share target by 2020. However, hourly matching issues between  
551 supply and demand of an exemplary building within the campus showed that only electrical  
552 equipment loads can be partially matched on an hourly basis (for around 22% of the time  
553 under peak production conditions namely). In such cases, the use of the devised method can  
554 help inform the choice of a suitable strategy to better exploit BIPV potentialities such as the  
555 supply from the grid or from nearby buildings, or the adoption of an energy storage system.

556

### 557 **Acknowledgements**

558 The presented work was developed within the framework of project 'REELCOOP - Research  
559 Cooperation in Renewable Energy Technologies for Electricity Generation', funded by the  
560 European Commission (FP7 ENERGY.2013.2.9.1, Grant agreement no: 608466). The  
561 authors would like to thank Ms. Elena Rico, Mr. Juan Luis Lechón and Mr. Teodosio del  
562 Caño from Onyx Solar for their technical assistant.

563

### 564 **References**

565 ANSI/ASHRAE, 2002. ASHRAE Guideline 14-2002 Measurement of Energy and Demand

566 Savings. Ashrae 8400, 170.

- 567 ASHRAE Standard 90.1-2004. Energy standard for buildings except low-rise residential  
568 buildings. Atlanta: ASHRAE; 2004
- 569 ASHRAE Standard 90.2-2004. Energy-efficient design of low-rise residential buildings.  
570 Atlanta: ASHRAE; 2004.
- 571 ASHRAE, ASHRAE Handbook - Fundamentals, Atlanta, GA, USA, 2005.
- 572 ASHRAE, ASHRAE Handbook Fundamentals, American Society of Heating, Refrigerating  
573 and Air-Conditioning Engineers, Inc., Atlanta, 2009.
- 574 ASTM G173-03, Standard Tables for Reference Solar Spectral Irradiances: Direct Normal  
575 and Hemispherical on 37° Tilted Surface (2012).
- 576 Baljit, S.S.S., Chan, H.-Y., Sopian, K., 2016. Review of building integrated applications of  
577 photovoltaic and solar thermal systems. *J. Clean. Prod.* 137, 677–689.  
578 doi:10.1016/j.jclepro.2016.07.150
- 579 Biljecki, F., 2013. The Concept of Level of Detail in 3D City Models – PhD Research  
580 Proposal. GIS Report No. 62. TU Delft. <<http://www.gdmc.nl/publications/reports/GIS62.pdf>> (accessed June 2017)
- 581 Biyik, E., Araz, M., Hepbasli, A., Shahrestani, M., Yao, R., Shao, L., Essah, E., Oliveira,  
582 A.C., del Caño, T., Rico, E., Lechón, J.L., Andrade, L., Mendes, A., Atlı, Y.B., 2017. A  
583 key review of building integrated photovoltaic (BIPV) systems. *Eng. Sci. Technol. an*  
584 *Int. J.* 20, 833–858. doi:10.1016/j.jestch.2017.01.009
- 585 Brito, M.C., Freitas, S., Guimaraes, S., Catita, C., Redweik, P., 2017. The importance of  
586 facades for the solar PV potential of a Mediterranean city using LiDAR data. *Renew.*  
587 *Energy* 111, 85–94. doi:10.1016/j.renene.2017.03.085
- 588 Brownsword, R.A., Fleming, P.D., Powell, J.C., Pearsall, N., 2005. Sustainable cities -  
589 Modelling urban energy supply and demand. *Appl. Energy* 82, 167–180.  
590 doi:10.1016/j.apenergy.2004.10.005
- 591

- 592 Compagnon, R., 2004. Solar and daylight availability in the urban fabric. *Energy Build.* 36,  
593 321–328. doi:10.1016/j.enbuild.2004.01.009
- 594 Cucchiella, F., D’Adamo, I., Lenny Koh, S.C., 2015. Environmental and economic analysis  
595 of building integrated photovoltaic systems in Italian regions. *J. Clean. Prod.* 98, 241–  
596 252. doi:10.1016/j.jclepro.2013.10.043
- 597 De La Flor, F.J.S., Cebolla, R.O., Félix, J.L.M., Domínguez, S.Á., 2005. Solar radiation  
598 calculation methodology for building exterior surfaces. *Sol. Energy* 79, 513–522.  
599 doi:10.1016/j.solener.2004.12.007
- 600 DIVA software, <http://solemma.net/Diva.html> (accessed June 2017)
- 601 Dogan, T., Reinhart, C., Michalatos, P., 2015. Autozoner: an algorithm for automatic thermal  
602 zoning of buildings with unknown interior space definitions. *J. Build. Perform. Simul.*  
603 1493, 1–14. doi:10.1080/19401493.2015.1006527
- 604 Erdélyi, R., Wang, Y., Guo, W., Hanna, E., Colantuono, G., 2014. Three-dimensional SOLar  
605 RADIation Model (SORAM) and its application to 3-D urban planning. *Sol. Energy* 101,  
606 63–73. doi:10.1016/j.solener.2013.12.023
- 607 Esclapés, J., Ferreiro, I., Piera, J., Teller, J., 2014. A method to evaluate the adaptability of  
608 photovoltaic energy on urban fa??ades. *Sol. Energy* 105, 414–427.  
609 doi:10.1016/j.solener.2014.03.012
- 610 EU, 2010. Directive 2010/31/EU of the European Parliament and of the Council of 19 May  
611 2010 on the energy performance of buildings (recast). *Off. J. Eur. Union* 13–35.  
612 doi:doi:10.3000/17252555.L\_2010.153.eng
- 613 European Parliament, 2009. Directive 2009/28/EC of the European Parliament and of the  
614 Council of 23 April 2009. *Off. J. Eur. Union* 140, 16–62.  
615 doi:10.3000/17252555.L\_2009.140.eng
- 616 Fath, K., Stengel, J., Sprenger, W., Wilson, H.R., Schultmann, F., Kuhn, T.E., 2015. A

- 617 method for predicting the economic potential of (building-integrated) photovoltaics in  
618 urban areas based on hourly Radiance simulations. *Sol. Energy* 116, 357–370.  
619 doi:10.1016/j.solener.2015.03.023
- 620 Freitas, S., Catita, C., Redweik, P., Brito, M.C., 2015. Modelling solar potential in the urban  
621 environment: State-of-the-art review. *Renew. Sustain. Energy Rev.* 41, 915–931.  
622 doi:10.1016/j.rser.2014.08.060
- 623 Jakubiec, J.A., Reinhart, C.F., 2013. A method for predicting city-wide electricity gains from  
624 photovoltaic panels based on LiDAR and GIS data combined with hourly Daysim  
625 simulations. *Sol. Energy* 93, 127–143. doi:10.1016/j.solener.2013.03.022
- 626 Kaplani, E., Kaplanis, S., 2014. Thermal modelling and experimental assessment of the  
627 dependence of PV module temperature on wind velocity and direction, module  
628 orientation and inclination. *Sol. Energy* 107, 443–460.  
629 doi:10.1016/j.solener.2014.05.037
- 630 Kim, B., Kim, K., Kim, C., 2017. Determining the optimal installation timing of building  
631 integrated photovoltaic systems. *J. Clean. Prod.* 140, 1322–1329.  
632 doi:10.1016/j.jclepro.2016.10.020
- 633 Loveday, D.L., Taki, A.H., 1996. Convective heat transfer coefficients at a plane surface on a  
634 full-scale building facade, *International Journal of Heat and Mass Transfer*, 39, 1729-  
635 1742
- 636 Lund, P., 2012. Large-scale urban renewable electricity schemes - Integration and interfacing  
637 aspects. *Energy Convers. Manag.* 63, 162–172. doi:10.1016/j.enconman.2012.01.037
- 638 Mardaljevic, J., 2000. *Daylight Simulation: Validation, Sky Models and Daylight*  
639 *Coefficients* - PhD Research.
- 640 Martínez-Rubio, A., Sanz-Adan, F., Santamaría-Peña, J., Martínez, A., 2016. Evaluating  
641 solar irradiance over facades in high building cities, based on LiDAR technology. *Appl.*

- 642 Energy 183, 133–147. doi:10.1016/j.apenergy.2016.08.163
- 643 Mattei, M., Notton, G., Cristofari, C., Muselli, M., Poggi, P., 2006. Calculation of the  
644 polycrystalline PV module temperature using a simple method of energy balance.  
645 Renew. Energy 31, 553–567. doi:10.1016/j.renene.2005.03.010
- 646 Palyvos, J.A., 2008. A survey of wind convection coefficient correlations for building  
647 envelope energy systems' modeling. Appl. Therm. Eng. 28, 801–808.  
648 doi:10.1016/j.applthermaleng.2007.12.005
- 649 Perez, R., Seals, R., Ineichen, P., Stewart, R., Menicucci, D., 1987. A new simplified version  
650 of the perez diffuse irradiance model for tilted surfaces. Sol. Energy 39, 221–231.  
651 doi:10.1016/S0038-092X(87)80031-2
- 652 Redweik, P., Catita, C., Brito, M., 2013. Solar energy potential on roofs and facades in an  
653 urban landscape. Sol. Energy 97, 332–341. doi:10.1016/j.solener.2013.08.036
- 654 Reinhart, C., Rakha, T., Weissman, D., 2014. Predicting the Daylit Area—A Comparison of  
655 Students Assessments and Simulations at Eleven Schools of Architecture. Leukos 10,  
656 193–206. doi:10.1080/15502724.2014.929007
- 657 Reinhart, C.F., Cerezo Davila, C., 2016. Urban building energy modeling - A review of a  
658 nascent field. Build. Environ. 97, 196–202. doi:10.1016/j.buildenv.2015.12.001
- 659 Reinhart, C.F., Dogan, T., Jakubiec, J.A., Rakha, T., Sang, A., 2013. Umi - an Urban  
660 Simulation Environment for Building Energy Use , Daylighting and Walkability. Proc.  
661 BS2013 13th Conf. Int. Build. Perform. Simul. Assoc. 476–483.
- 662 Ross, R. G., J., 1976. Interface design considerations for terrestrial solar cell modules. 1976  
663 Photovolt. Spec. Conf. 801–806.
- 664 Schwingshackl, C., Petitta, M., Wagner, J.E., Belluardo, G., Moser, D., Castelli, M., Zebisch,  
665 M., Tetzlaff, A., 2013. Wind effect on PV module temperature: Analysis of different  
666 techniques for an accurate estimation. Energy Procedia 40, 77–86.

- 667 doi:10.1016/j.egypro.2013.08.010
- 668 Shahrestani, M., Yao, R., Essah, E., Shao, L., Oliveira, A.C., Hepbasli, A., Biyik, E., Caño,  
669 T. del, Rico, E., Lechón, J.L., 2017. Experimental and numerical studies to assess the  
670 energy performance of naturally ventilated PV façade systems. *Sol. Energy* 147, 37–51.  
671 doi:10.1016/j.solener.2017.02.034
- 672 Skoplaki, E., Boudouvis, A.G., Palyvos, J.A., 2008. A simple correlation for the operating  
673 temperature of photovoltaic modules of arbitrary mounting. *Sol. Energy Mater. Sol.*  
674 *Cells* 92, 1393–1402. doi:10.1016/j.solmat.2008.05.016
- 675 Tong, Z., Whitlow, T.H., Landers, A., Flanner, B., 2016. A case study of air quality above an  
676 urban roof top vegetable farm. *Environ. Pollut.* 208, 256–260.  
677 doi:10.1016/j.envpol.2015.07.006
- 678 Turkey Energy efficient report,  
679 <https://library.e.abb.com/public/bcfe8957cb2c8b2ac12578640051cf04/Turkey.pdf>  
680 (accessed November 2017).
- 681 US Department of Energy. EnergyPlus version 8.1.  
682 <http://apps1.eere.energy.gov/buildings/energyplus/>(accessed June 2017)
- 683 Ward, G.J., Rubinstein, F.M., 1988. A new technique for computer simulation of illuminated  
684 spaces. *J. Illum. Eng. Soc.* doi:10.1080/00994480.1988.10748710
- 685 Wegertseder, P., Lund, P., Mikkola, J., García Alvarado, R., 2016. Combining solar resource  
686 mapping and energy system integration methods for realistic valuation of urban solar  
687 energy potential. *Sol. Energy* 135, 325–336. doi:10.1016/j.solener.2016.05.061
- 688 Wilcox, S., Marion, W., 2008. Users manual for TMY3 data sets. *Renew. Energy* 51.  
689 doi:NREL/TP-581-43156
- 690
- 691

**Highlights:**

- A bottom-up approach to estimate BIPV electricity yield in urban buildings;
- Python-based algorithm editor Grasshopper is used to interconnect simulation tools;
- Comparison of electricity supply and demand informs about matching issues;
- The approach has been tested for a real case study in Yasar University, Turkey;
- BIPV system could achieve an annual renewable share of 23% under BAU scenario.